Training-Aided Frequency Offset Estimation in 16-QAM Nyquist Transmission Systems

Fabio Pittalà[(1,2)], Josef A. Nossek[(2)]

(1) European Research Center, Huawei Technologies Duesseldorf GmbH, Riesstrasse 25, D-80992 Munich, Germany,
(2) Institute for Circuit Theory and Signal Processing, Technische Universität München, Arcisstr. 21, D-80290 Munich, Germany.
fabio.pittala@huawei.com

***Abstract*— We propose a novel training-aided feed-forward frequency-offset estimation method based on CAZAC sequences. The precision and robustness of the estimator is evaluated with respect to CD and PMD for frequency offsets up to ±3.6 GHz.**

Fiber Optics Communications; Coherent Communications; Optical Performance Monitoring; Frequency Offset.

I. Introduction

Coherent detection in combination with digital signal processing (DSP) allowing for efficient channel impairments mitigation have revolutionized the design and operation of optical fiber communication systems [1]. DSP can employ either non-training-aided (NTA) or training-aided (TA) algorithms, where the latter guarantee reduction of complexity, higher performance stability and transparency with respect to the modulation-format of the user data [2-4]. Particularly, TA channel estimation (CE) is superior to NTA adaptive methods when it comes to separation of the different streams in multiple-input multiple-output (MIMO) systems [5]. TA algorithms acquire the channel by comparing the transmitted and the received training symbols [6-7]. The main drawback of TA-CE is the high sensitivity to the frequency offset (FO) due to the mismatch between the laser frequencies used by the transmitter and the receiver. Therefore, accurate FO estimation (FOE) and compensation is required before performing TA-CE [8-10].

In this paper, we present a feed-forward TA-FOE method which uses the same training sequences (TS) employed for CE in a 256 Gb/s polarization-division multiplexed (PDM) 16-level quadrature amplitude modulation (QAM) transmission system with Nyquist pulse shaping. The proposed method is verified for different TS schemes based on constant amplitude zero-autocorrelation (CAZAC) code. The precision and robustness of the FOE is investigated with respect to chromatic dispersion (CD) and polarization-mode dispersion (PMD).

II. Training-Aided Frequency Offset Estimation

The proposed TA-FOE is based on the estimated 2×2 MIMO channel transfer function $\mathbf{h}[n] = \begin{bmatrix} h_{xx}[n] & h_{xy}[n] \\ h_{yx}[n] & h_{yy}[n] \end{bmatrix}$. The TS to estimate such channel can be composed of two independent blocks $c_x[n] = c[n]$ and $c_y[n] = c[n + N/2]$ transmitted simultaneously one per polarization (Single-Block (SB)-TS); or of four independent blocks $c_{x,1}[n] = c[n]$, $c_{y,1}[n] = c[n + N/2]$, $c_{x,2}[n] = -c^*[n + N/2]$ and $c_{y,2}[n] = c^*[n]$ transmitted two per polarization (Double-Block (DB)-TS), where $c[n]$ is a perfect-square minimum-phase (PS-MP) CAZAC sequence of length N symbols. Each block $c[n]$ is surrounded by a couple of guard intervals of length $N/2$ symbols. With the aid of the received spectra and the known transmitted spectra of the TS, the receiver calculates the zero-forcing (ZF) CE as described in [6] (without time-domain windowing) for SB-TS and as described in [7] for DB-TS. The cost function of the TA-FOE is given by:

$$CF_{\Delta_{FO}} = \sum_{n=1}^{N} \left|h_{\Delta_{FO}}^{xx}[n]\right| + \sum_{n=1}^{N} \left|h_{\Delta_{FO}}^{xy}[n]\right| + \sum_{n=1}^{N} \left|h_{\Delta_{FO}}^{yx}[n]\right| + \sum_{n=1}^{N} \left|h_{\Delta_{FO}}^{yy}[n]\right|$$

where Δ_{FO} is the FO digitally applied to reference CAZAC block $c_{i,\Delta_{FO}}[n] = c_i[n] \cdot e^{-j2\pi\Delta_{FO}t}$ with $i \in \{x, y\}$. The parameter Δ_{FO} is selected from a set of expected FO values. The cost function $-CF_{\Delta_{FO}}$ for FOE based on SB-TS and DB-TS is

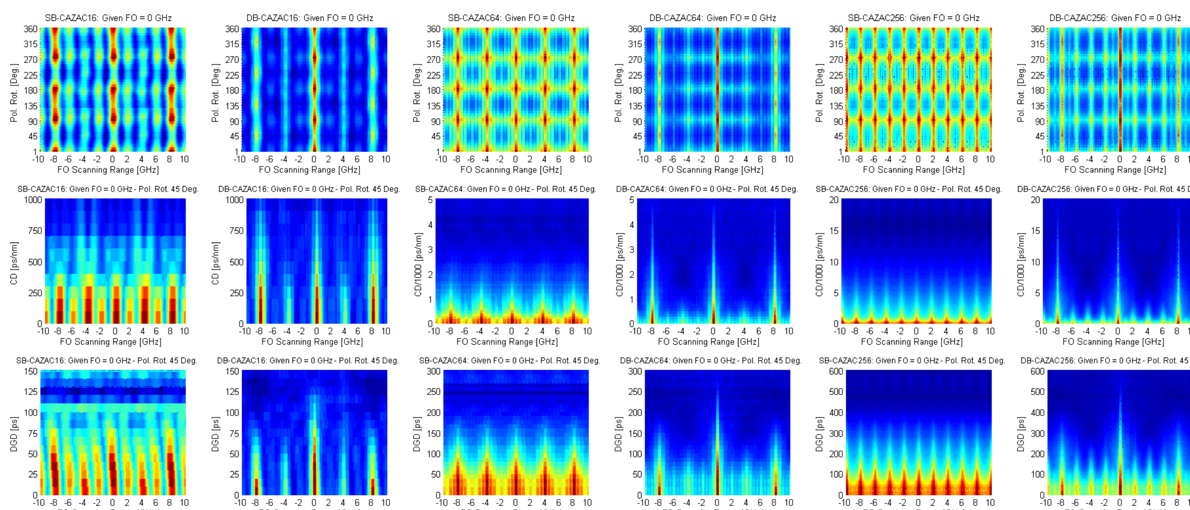

Fig.1 TA-FOE Cost Function (Baudrate equal to 32 GB).

plotted in Fig. 1. The maximum value of $-CF_{\Delta_{FO}}$ corresponds to the FO Δ_{FO} present in the system. The length N of the PS-MP CAZAC block is chosen to be equal to 16, 64 and 256 symbols. The first row in Fig.1 shows that the FOE is limited to FO values in between $\pm B/4$ for CE based on DB-TS and in between $\pm B/\sqrt{N}$ for CE based on SB-TS, where B is the signal baudrate. Considering $B = 32$ GB FOE based on DB-TS covers FO values in between ± 4 GHz independently from the value N. Instead, FOE based on SB-TS covers FO values in between ± 4 GHz, ± 2 GHz and ± 1 GHz for values of N equal to 16, 64 and 256 symbols, respectively. The second and the third row of Fig.1 show the behavior of $-CF_{\Delta_{FO}}$ for estimation based on TS impaired by CD and differential group delay (DGD), respectively.

III. Simulation Results

The evaluation of the proposed algorithm is based on a 32 GB PDM Nyquist (with roll off factor equal to 0.01) system with 16-QAM leading to a transmission rate of 256 Gb/s. The lasers used in the system have a linewidth of 100 kHz. Simulations of the linear channel include residual CD, first-order PMD, polarization rotation angle and polarization phase. At the receiver, white Gaussian noise is loaded onto the signal, followed by an optical Gaussian band-pass filter (4th-order, double-sided 40 GHz), the polarization-diverse 90°-hybrid and an electrical

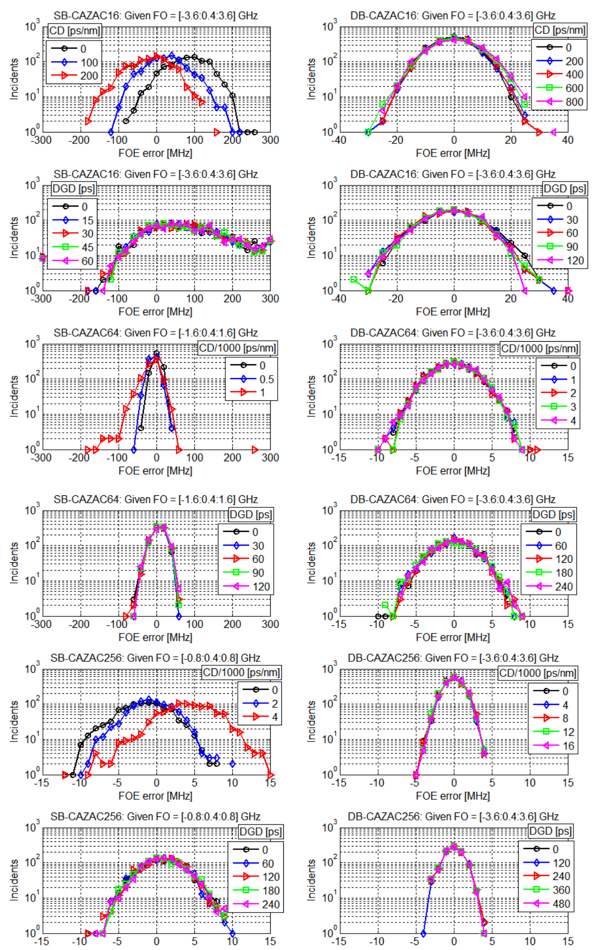

Fig.2 TA-FOE Performance Evaluation.

Bessel filter (5th-order, 16 GHz). A 64 Gsamples/s analog-to-digital-converter (ADC) stage digitalizes the received signal at 2 samples per symbol. The TS are inserted in between the user data forming frames with ~2% overhead. Frame synchronization is assumed to be ideal. The TA-FOE does not require averaging between consecutive TS [7]. The FOE scanning step is set to 1 MHz. For FOE based on DB-TS the FO scanning range is defined between ± 3.8 GHz. For FOE based on SB-TS the FO scanning range is set between ± 3.8 GHz, ± 1.8 GHz, ± 0.9 GHz for N equal to 16, 64 and 256 symbols, respectively.

Fig. 2 shows the distribution of the TA-FOE errors represented by histograms which demonstrate the precision and robustness of the proposed algorithm, as function of CD and DGD. For FOE based on DB-TS the given FO is varied between ± 3.6 GHz. For FOE based on SB-TS given FO is varied between ± 3.6 GHz, ± 1.6 GHz, ± 0.8 GHz for N equal to 16, 64 and 256 symbols, respectively. The FO is increased in step of 0.4 GHz. The CD and DGD range is chosen depending on the TS scheme and its length N, Fig. 1. For any value of FO and CD or DGD, 100 simulations have been performed with random polarization rotation angle and polarization phase chosen between 0° and 360°.

DB-TS based FOE allows precise and accurate estimation over a large range of CD and DGD. For TS with $N = 16$ symbols the FOE tolerate CD up to 800 ps/nm and DGD up to 120 ps with FOE error below ± 40 MHz. For TS with $N = 64$, the CD and DGD tolerance increases up to 4000 ps/nm and 240 ps, respectively, while the maximum FOE error reduces to ± 10 MHz. The best performances are obtained for TS with $N = 256$, where CD up to 16000 ps/nm and DGD up to 480 ps can be tolerated with FOE error between ± 5 MHz.

In contrast, SB-TS based FOE exhibits poor performances. For TS with $N = 16$ symbols the FOE fails. For $N = 64$, the FOE tolerate CD up to 1000 ps/nm and DGD up to 120 ps. However, the TA-FOE range is limited to ± 1.6 GHz and a large FOE error between ± 300 MHz is experienced. For $N = 256$, although the FOE range is further reduced to ± 0.8 GHz, acceptable FOE is obtained. The maximum estimation error is now confined between ± 15 MHz with tolerated CD up to 4000 ps/nm and DGD up to 240 ps.

IV. Conclusions

A novel frequency offset estimation method based on CAZAC sequences has been demonstrated in a PDM 16-QAM Nyquist transmission system. The proposed estimator covers frequency offsets between ± 3.6 GHz and with an appropriate training sequence shows high tolerance with respect to residual CD (up to ~16000 ps/nm) and DGD (up to ~480 ps). The estimator has zero mean value and maximum error between ± 5 MHz.

References

[1] S. Savory, Optical Express, **16**, 804-817 (2008).
[2] M. Kuschnerov, et al., IEEE Photonics Journal, **2**, 3, 387-403 (2010).
[3] B. Spinnler, IEEE Journal of Selected Topics in Quantum Electronics, **16**, 5, 1180-1192 (2010).
[4] F. Pittalà, et al., OFC'12, OM2H.4 (2012).
[5] B. Spinnler, et al., OFC'13, OW4B.3 (2013).
[6] F. Pittalà, et al., SPPCom'12, SpTu3A.4 (2012)
[7] F. Pittalà, et al., ICTON'11, We.D1.5 (2011).
[8] R. Elschner, et al., ECOC'12, We.1.A.4 (2012)
[9] C. Zhu, et al., OFC'13, OW4B.5 (2013).
[10] C. Zhu, et al., OFC'13, OW4B.7 (2013).